Available online at www.sciencedirect.com
SCIENCE DIRECT®
ELSEVIER
Journal of Photochemistry and Photobiology A: Chemistry 157 (2003) 47–53
Journal of Photochemistry and Photobiology A:Chemistry
www.elsevier.com/locate/jphotochem

Synthesis of photocatalytic TiO_2 nanoparticles: optimization of the preparation conditions

Yassine Bessekhouad, Didier Robert*, Jean Victor Weber

Laboratoire de Chimie et Applications (EA 3471), Université de Metz, Rue Victor Demange,
57500 Saint-Avold, France

Received 20 January 2003; received in revised form 20 January 2003; accepted 29 January 2003

Abstract

Nanosized titanium oxide (TiO_2) powders were prepared by sol–gel route. The preparation parameters are optimized by means of Malachite green oxalate degradations. All catalysts were analyzed by X-ray diffraction (XRD) and BET technique. The best catalyst was compared to TiO_2-P25 using two other types of pollutant, 4-hydroxy benzoic and benzamide (BZ) and their performance was found to be strongly dependant on the pollutant's type.

Keywords: Titanium dioxide; Photocatalysis; Sol–gel route; Nanosized particle

1. Introduction

Photoassisted organic pollutants degradations induced by illumination of suspensions containing small particles of semi-conducting oxides continue to attract great attention as an alternative technology for wastewater treatment and are a subject of many investigations [1–8].

The photoelectrochemical energy conversion depends on the efficient spatial separation and subsequent interfacial charge transfer of electrons and positively charged holes (the two charges carriers) that are created by the absorption of photons in the semiconductor or by the molecules at semiconductor-molecules interfaces. The separated electrons and holes drive electrochemical oxidation–reduction reactions with the redox molecules at the semiconductor surface.

Semiconductors used for such applications must have a high resistance to photocorrosion, water hydrolysis processes and low coast. Their photosensitivity must be efficient when using the solar spectrum and have a high quantum efficiency. However, the material having this ideal property has not been obtained.

It is well known that TiO_2 is the promising material as semi-conductor having high photochemical stability and low cost. TiO_2 is used for different environmental applications, such as, photocatalytic degradations of various organic contaminants into non toxic compounds like water, CO_2 and diluted mineral acid [3–5], removing heavy metal ions from the solution and converting them into less toxic ones [9] and water photosplitting into H_2 and O_2 [10,11].

In the recent years, scaling optical and electronic properties of nanomaterials which become strongly size dependant focused attention on the preparation of nanoparticle semi-conductors [12]. TiO_2 nanoparticles in powder have real advantages in relation to photocatalytic activity. In order to do this, several methods of preparation have been reported, e.g. sol–gel organic or inorganic method [13], hydrothermal method [14] and hydrolysis of inorganic salt [15].

This work is devoted to the study of the influence of different parameters like methanol and water ratios, temperature and time of the refluxed process, on the preparation of TiO_2 nanoparticles. The photocatalytic efficiency of these materials was evaluated using Malachite green as pollutant.

2. Experimental

2.1. Preparation of TiO_2 nanoparticles

The following commercial reagents were used without any further purifications: tetraisopropylorthotitanate $Ti(OC_3H_7)_4$, purity 99%; ethanol (EtOH) absolute grade, purity 99.9%; methanol (MeOH) absolute grade, purity 99.9%; hydroxypropyl cellulose P.M. 100.000 (HPC);

---

* Corresponding author. Tel.: +33-3879-39108; fax: +33-3879-39101.
E-mail address: drobert@iut.univ-metz.fr (D. Robert).

1010-6030/03/$ – see front matter © 2003 Published by Elsevier Science B.V.
doi:10.1016/S1010-6030(03)00077-7

TiO_2-P25, purity 99.8% (Degussa Corporation). Malachite green oxalate (Réactifs RAL, France); 4-hydroxy benzoic acid (Aldrich); Benzamide (Aldrich).

2.1.1. Method 1

TIPT and CHD were dissolved in 300 ml of absolute EtOH with the molar ratio (1:1). The reaction mixture was stirred at 80 °C for 3 h. After cooling, a controlled amount of water was added dropwise to the solution.

2.1.2. Method 2

TIPT was slowly added to a basic solution (pH $\sim$ 9) of hydrogen peroxide H_2O_2 (200 ml, 3.6 M) under stirring at 5 °C. The yellow gel observed indicates the formation of a peroxide complex of Titanium.

2.1.3. Method 3

This is a variation of method 2, where the peroxide complex of Ti is substituted by a complex obtained by dissolution of TIPT in TEA (TEA/TIPT molar ratio: 0.5). The initial pH of solutions obtained from the method 1–3 were adjusted to 6 by NH_4OH or HNO_3, and then dispersed in 100 ml of hexane with the presence of surfactant (Agar–Agar) 10^{-2} g/ml as emulsifying agents. After gelation, stirring was continued for 1 h. The gel was filtered and washed subsequently by water (500 ml) and EtOH (200 ml), dried at room temperature for 12 h.

2.1.4. Method 4

In order to get nanostructured TiO_2, $Ti(OC_3H_7)_4$ ($Ti(OR)_4$) solution was dissolved in mixture of MeOH and EtOH at different molar ratios and agitated at 65 °C during 3 h under magnetic stirrer. Water was added dropwise into the hot solution (65 °C) during this period of time. The molar concentration of each species is related to the concentration of alkoxide group (OR). The precipitate is isolated by filtration, washed with hot water and organic solvents to remove the adsorbed impurities, and heated at 110 °C for 12 h.

2.1.5. Method 5

$TiCl_4$ was added dropwise and under stirring to 500 ml of water at about 0 °C. The colloidal TiO_2 solution was dialyzed until the pH lay between 2 and 3. The solvent was removed by rotary evaporation.

2.1.6. Method 6

The present method of synthesis is an adaptation of the method used by Kim and Kim [16] for the preparation of TiO_2 nanosized using a two-stage mixed method. The starting solution containing water 70% and alcohol 30% (MeOH and EtOH in the ratio 1:10) was added dropwise to a solution containing: TIPT + HPC + alcohol. Thereafter, the mixture resulting at the first stage was agitated for 60 min under Ar atmosphere. When the first stage reaction (semi-bath) was finished, the bath reaction (the second stage) was started. Two solutions containing respectively (water + alcohol) and (TIPT, HPC, alcohol) were added to the solution obtained from the first stage. The resulting mixture was vigorously stirred during 60 min. The powders were isolated by repeated centrifugation and dried at 70 °C for 12 h.

All obtained products were treated at 550 °C for 2 or 10 h in air [17].

2.2. Characterization

X-ray diffraction (XRD) patterns are collected at 295 K using Cu Kα ($\lambda = 0.15418$ nm) radiation and were used to determine the identity of any phase present and their crystallite size. The crystalline phase can be determined from integration intensities of anatase (1 0 1), rutile (1 1 0) and brookite (1 2 1) peaks. If a sample contains only anatase and rutile, the mass fraction of rutile (χ) can be calculated from the following equation [18].

$$\chi = \frac{I_R}{0.8 I_A + I_R}$$

where I_A and I_R represent the integrated intensity of the anatase (1 0 1) and rutile (1 1 0) peaks, respectively.

The average crystallite sizes of anatase and rutile were determined according to the Scherer equation using the FWHM data of each phase after correcting the instrument broading. The specific areas were determined by BET isotherms using N_2 at 77 K.

2.3. Photocatalytic activity

Malachite green (MG), benzamide (BZ) and 4-hydroxybenzoic acid (4-HBZ) were taken as representative pollutants resulting from textile industry, pesticide and olive oil extractions and can be considered as highly contaminant wastewater.

For the simplicity of its analysis and its quick degradation process in the presence of TiO_2 as photocatalyst, MG was used as pollutant for TiO_2 optimization procedure. Solar box ATLAS Suntest *CPS+* simulating natural radiation equipped with vapour Xenon lamp ($300\,\text{nm} < \lambda < 800\,\text{nm}$) was used in all experiments. In each run, 125 mg of TiO_2 was dissolved in 250 ml of MG (10 mg/l) solutions. The mixture was sonicated before irradiation for 2 min. To obtain highly dispersed catalysts and agitated in the dark for 1 h before irradiation procedure. At given irradiation time intervals, the samples (5 ml) were taken out and then analyzed by UV-Vis spectrophotometer “Shimadzu PC1201” (maximum absorbance was taken at 618 nm). For BZ and 4-HBZ degradations, typically 500 mg of TiO_2 was dissolved in 500 ml of such solutions (20 mg/l BZ, 30 mg/l 4-HBZ). During the irradiation procedure, 10 ml of solution were regularly taking, filtered (Watmann, 0.45 μm) and followed by HPLC equipped by a C18 column to calculate the remaining concentrations.

3. Results and discussion

3.1. Preliminary results

In the previous work [17], we have selected in the literature six different methods of TiO_2 nanoparticles preparation. The prepared TiO_2 materials have been characterized by XRD and BET analysis and by scanning electron microscopy (SEM). A thermal treatment is necessary to improve the crystallinity of amorphous compounds. When TiO_2 powders are calcinated at higher temperature, crystal structure transformations may occur. The amorphous-anatase and anatase-rutile transitions depend strongly on the method of preparation, the nature of the precursor and calcination conditions.

Typically, the XRD patterns for different products calcinated at 550 °C for 10 h were found to be more crystallized than the same products calcinated at 550 °C for 2 h. These compounds indicate different stages of crystallization, depending on the nature of the precursor and the procedure of preparation. Furthermore, the samples prepared from the organic precursors presented more ability to form a high crystallinity than the samples generated from mineral precursors. In all cases, the particle size does not exceed 40 nm and the smaller crystallite was obtained with method 1 (Table 1). A good specific surface was also obtained by this method (44.5 m^2/g) compared with other methods that can not exceed ∼20 m^2/g.

The SEM observation showed high homogeneity of the samples prepared by method 1. The samples prepared with reflux process (method 4) showed two types of aggregates with a different average size [17].

The photoactivity of the prepared TiO_2 nanoparticles was investigated using benzamide (BZ). The photocatalytic activity of the samples treated at 550 °C for 10 h was found to be higher than the samples treated for 2 h [17]. This fact could be associated to the more crystalline structure observed for the samples calcinated for 10 h though this long treatment induces the decrease of the specific area.

In our case, the more influencing parameter is the level of crystallinity which can be concluded from the results of photocatalytic activity. The crystallinity and surface area are two parameters involving on different ways.

The products resulting from methods 2, 3 and 5 showed a low photoactivity. Indeed, this comportment is attributed to the poor crystallinity observed by X-ray analysis. The amorphous characters of compounds induce high concentrations of defects. Each one acts as a recombination center when electrons and holes were generated under illuminations [19]. The same photoactivity was obtained when TiO_2 from methods 6 and 1 were used though both compounds have different physical properties. The very low specific surface (6.8 m^2/g) is compensated by a high level of crytallinity for method 6 products. In addition, the interesting surface area obtained from method 1 (32.7 m^2/g) confer sufficiently active surface to compensate the moderate crystallinity. The very small crystallite size (∼10 nm) implies a high number of particles, each particle acts like nanophotochemical radical generator.

The effect of rutile-anatase distribution on photocatalytic activity of TiO_2 can be observed by using the product resulting from method 4. In fact, the best result of photoactivity was obtained close to that observed for TiO_2 P25 (30% of rutile and 70% of anatase powder). The higher crystallinity combined with good surface improve the photocatalytic performance. However, the surface area obtained from this new method of preparation is low in comparison to TiO_2-P25 (50 m^2/g).

It should be taken into account that this new method of preparation combining two alcohols has not been optimized. Nevertheless, the optimization of method 4 is the main objective of this work. It shows the high influence of methanol and water ratios, temperature and time of the refluxed process.

3.2. Optimization of the method 4

3.2.1. Effect of Methanol/alkoxy group of precursor (OR) molar ratio

Fig. 1 shows the variation of the rate constant of Malachite green photocatalytic degradation as a function of methanol/OR molar ratio (with R: *iso*-propyl). These constants were determined according to the kinetic equations of order 1 after 30 min of irradiation. We can see that the amount of methanol induces the variation of catalyst efficiency. In the low and high concentrations of methanol, the catalysts are very efficient. However, for the middle concentrations, the photoactivity of obtained catalysts decreases drastically.

Table 1
Physical properties of obtained TiO_2

Thermal treatment duration (h)		Method 1	Method 2	Method 3	Method 4	Method 5	Method 6
2	*L* (nm)	7.92	19.81	13.21	19.87	–	23.23
	S (m^2/g)	44.5	–	23.1	17.2	14.9	6.7
10	*L* (nm)	10.02	20.24	13.21	19.81	17.23	39.65
	S (m^2/g)	32.07	–	19.50	14.00	15.4	6.8
	Percentage of BZ degraded after 1 h	50	15	40	75	30	60

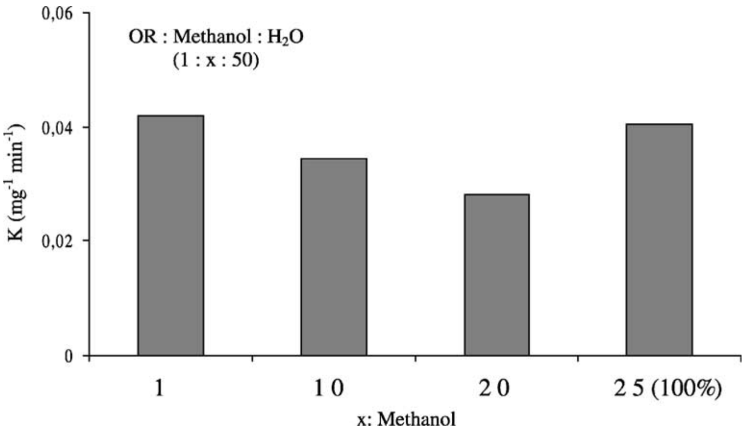

Fig. 1. Effect of methanol on photocatalytic activity of TiO_2 Malachite green as pollutant.

Table 2
XRD data of prepared TiO_2 samples with the preparation conditions

Nb of sample	OR:methanol:water ratios	Bath temperature (°C)	Refluxing time (h)	Amount of each phase[a]	Crystallite size[b]
1	1:1:50	65	3	*A*: 91.3, *R*: 8.7	D_A: 20.44, D_R: 41.06
2	1:20:50	65	3	*A*: 89.66, *R*: 10.34	D_A: 20.40, D_R: 20.53
3	1:1:1	65	3	*A*: 62.35, *R*: 37.66	D_A: 20.45, D_R: 25.66
4	1:1:75	65	3	*A*: 50.82, *R*: 49.18	D_A: 20.45, D_R: 25.66
5	1:1:75	55	3	*A*: 91.35, *R*: 8.65	D_A: 22.71, D_R: 13.68
6	1:1:75	67	3	*A*: 87.5, *R*: 12.50	D_A: 20.40, D_R: 25.66
7	1:1:75	75	9	*A*: 94.12, *R*: 5.88	D_A: 20.25, D_R: 20.52

[a] *A*: anatase phase and *R*: rutile phase.
[b] D_A: crystallite size of anatase and D_R: crystallite size of rutile.

If we compare the physical properties of the sample having the lowest photoactivity with the sample having the best photoactivity, only the grain sizes of rutile phase are different (Table 2). The amount of anatase and rutile phases is practically the same and no significant variation of surface area is observed (Table 3). Their surface areas were found to be very low. The conditions to prepare a better catalyst are selected for investigation of water effect (1:1).

3.3. *Effect of water*

The effect of the water amount used during the preparation procedures on the photoactivity of catalysts can be observed on Fig. 2. The photoactivity of catalysts is proportional to the amount of water used. The best result was obtained for the catalyst whose alkoxy-groups (OR) and water molar ratio was 1:75.

According to Livage et al. [20], the total sol–gel synthesis can be described by an alcoholic permutation reaction, hydrolysis, and condensation reactions, which are competitive with alkoxolation, oxolation and olation as follows:

(for our study, M: Ti^{4+}, R: *iso*-C_3H_7)

1. Alcoholic permutation

$$\mathrm{M(OR)}_z + x\mathrm{R'(OH)} \leftrightarrow \mathrm{M(OR)}_{z-x}(\mathrm{OR'})x + x\mathrm{ROH} \qquad (1)$$

2. Hydrolysis

$$\mathrm{M(OR)}_n + n\mathrm{H_2O} \leftrightarrow \mathrm{M(OH)}n + n\mathrm{ROH} \qquad (2)$$

3. Condensations reactions

Alcoxolation:

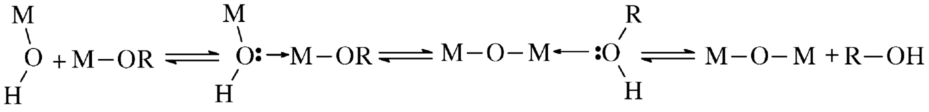

$$\overset{\mathrm{M}}{\underset{\mathrm{H}}{\mathrm{O}}} + \mathrm{M{-}OR} \rightleftharpoons \overset{\mathrm{M}}{\underset{\mathrm{H}}{\mathrm{O}}}{:}\rightarrow \mathrm{M{-}OR} \rightleftharpoons \mathrm{M{-}O{-}M} \leftarrow {:}\overset{\mathrm{R}}{\underset{\mathrm{H}}{\mathrm{O}}} \rightleftharpoons \mathrm{M{-}O{-}M} + \mathrm{R{-}OH} \qquad (3)$$

Oxolation:

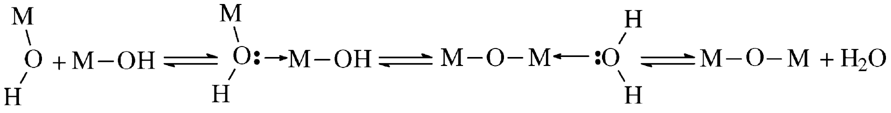

$$\overset{\mathrm{M}}{\underset{\mathrm{H}}{\mathrm{O}}} + \mathrm{M{-}OH} \rightleftharpoons \overset{\mathrm{M}}{\underset{\mathrm{H}}{\mathrm{O}}}{:}\rightarrow \mathrm{M{-}OH} \rightleftharpoons \mathrm{M{-}O{-}M} \leftarrow {:}\overset{\mathrm{H}}{\underset{\mathrm{H}}{\mathrm{O}}} \rightleftharpoons \mathrm{M{-}O{-}M} + \mathrm{H_2O} \qquad (4)$$

Table 3
Surface and rate constant of MG degradation for the TiO_2 samples

Nb of sample	S_{BET} (m^2/g)	K ($mg\,min)^{-1}$
1	7.7	0.0419
2	4.9	0.0282
3	6.6	0.0298
4	7.4	0.0546
5	35	0.0429
6	24	0.0743
7	26.6	0.0495

Olation:

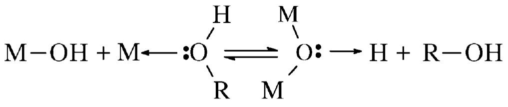

$$\mathrm{M{-}OH + M{\leftarrow}{:}\overset{H}{\underset{R}{O}} \rightleftharpoons \overset{M}{\underset{M}{O}}{:} \longrightarrow H + R{-}OH} \qquad (5)$$

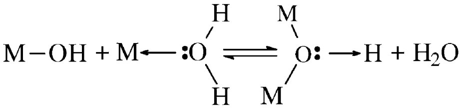

$$\mathrm{M{-}OH + M{\leftarrow}{:}\overset{H}{\underset{H}{O}} \rightleftharpoons \overset{M}{\underset{M}{O}}{:} \longrightarrow H + H_2O} \qquad (6)$$

The structure of the final gel depends on the relative contribution of alkoxolation (Eq. (3)), oxolation (Eq. (4)), and olation (Eqs. (5) and (6)), because these reactions develop the three-dimensional skeletons of titania. The amounts of water used during the gelation procedure determine the contribution of each reaction. For the low amount of water, hydrolysis of (Eq. (2)) rates are low and excess titanium alkoxide in the solvent favours the development of Ti–O–Ti chains through alcoxolation (Eq. (3)). Because each Ti is coordinated with four O atoms, the development of Ti–O–Ti chains results in three-dimensional polymeric skeletons with close packing. For a medium amount of water, high hydrolysis (Eq. (2)) rates favour the formation of $Ti(OH)_4$ and reduce the relative contribution of alcoxolation (Eq. (3)). Furthermore, the excess water suppresses the development of Ti–O–Ti chains by oxolation (Eq. (4)), because chemical equilibrium favours the creation of Ti–OH species. As a result, the first-order particles are loosely packed due to the presence of a large quantity of Ti–OH and insufficient development of three-dimensional polymeric skeletons.

For high concentration of water, the large excess of water favours the formation of $Ti(OH)_4O^+H_2$ by the coordination of water to $Ti(OH)_4$ (solvation phenomenon). This result in reactive $Ti–HO^+–Ti$ species can contribute to

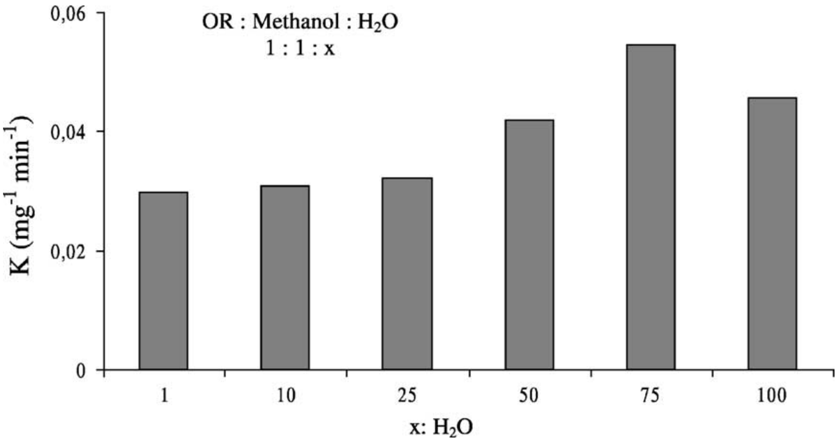

Fig. 2. Effect of H_2O on photocatalytic activity of TiO_2 Malachite green as pollutant.

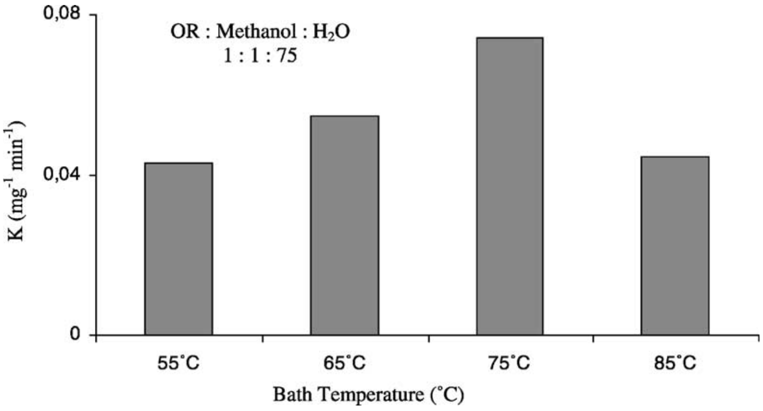

Fig. 3. Effect of bath temperatures on photocatalytic activity of TiO_2 Malachite green as pollutant.

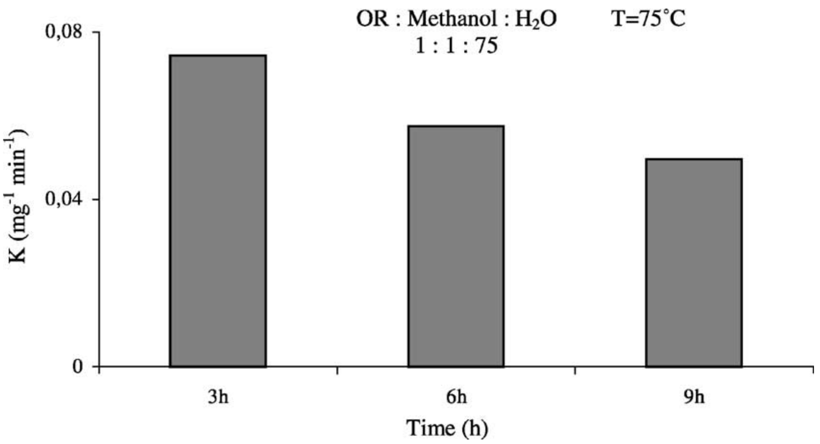

Fig. 4. Effect of gel formation time on photocatalytic activity of TiO_2 Malachite green as pollutant.

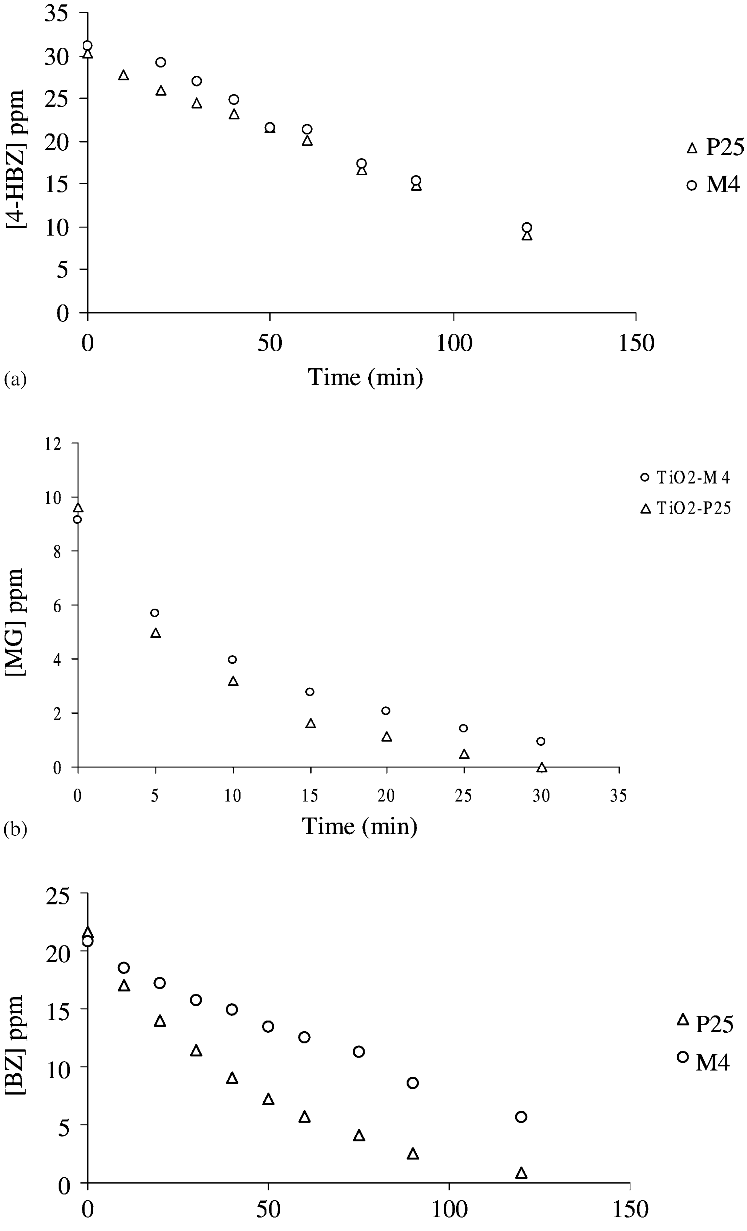

Fig. 5. Photocatalytic activity of optimized TiO_2: (a) 4-hydroxy benzoic acid; (b) Malachite green; (c) benzamide.

the development of polymeric Ti–O–Ti chains through the olation reaction (Eq. (6)). Thus, a three-dimensionally developed gel skeleton again yields closely packed first-order particles. Although excess water favours the formation of Ti–OH species by chemical equilibrium, the formed Ti–O^+H–H species are very reactive and quickly condense on other Ti–OH with production of water (Eq. (6)) or alcohol (Eq. (5)) to yield Ti–O–Ti chains. In brief, the amount of water used during the gelation procedure is determinant in terms of reaction mechanism occurring during the gel formation. As a consequence, the amount of active sites is tribute to the water amount.

3.4. *Effect of temperature and gel formation time*

Fig. 3 shows the effect of bath temperature on photocatalytic activity of final product. The constant rate of degradation increases with the temperature until 75 °C. At 75 °C, the best photoactivity was obtained. This temperature is greater than temperature of solvent evaporations (ethanol and methanol). When the bath temperature is equal to 85 °C, the constant rate of degradation decreases. The effect of refluxing time was investigated at 75 °C and it can be observed that 3 h under reflux are enough to produce a catalyst with interesting efficiency (Fig. 4).

In conclusion, the best conditions to prepare the best photocatalyst is the molar ratio 1:1:75, respectively, for OR:methanol:water during 3 h at 75 °C for the bath temperature.

3.5. *Catalyst efficiency as a function of degradated molecules*

The efficiency of optimized catalyst was studied as a function of three type organic pollutants: Malachite green oxalate as a dye, 4-hydroxy benzoic acid as an organic acids and benzamide as representative base.

Fig. 5 showed efficiency comparison between the optimized catalyst M4 and TiO_2-P25 versus each pollutant. For Malachite green oxalate degradations, the photoactivity of optimized catalyst was found to be close to that observed for TiO_2-P25. Using 4-hydroxy benzoic acid as pollutant, the photocatalytic activity of M4 is slightly weaker than TiO_2-P25. Unfortunately, when benzamide was used as pollutant, poor photoactivity was observed in comparison to TiO_2-P25. As a result, we can conclude that optimization of catalyst using only one molecule as pollutant is not sufficient. This fact is attributed to the development of certain affinity versus elimination of type pollutant that occurs during the optimization procedure. It is not evident to obtain catalyst having efficient use in all situations but the development of catalyst having high abilities to remove particular type of pollutant is more realists.

4. Conclusion

The research work presented in this paper leads us to draw the following conclusions. TiO_2 prepared by sol–gel route was optimized using Malachite green oxalate during photocatalytic test. The optimum conditions are obtained with the ratios 1:1:75 between alkoxide group of precursor, methanol, and H_2O. The mixture must be prepared in bath for 3 h at 75 °C. These conditions produced a better catalyst for Malachite green degradation. Moreover, when this catalyst was used for degradation of benzamide and 4-hydroxy benzoic acid, other efficiency was observed in comparison to TiO_2-P25. From all this results, we can conclude that optimization of one method using only one type of pollutant is not sufficient because the development of certain affinity occur between catalyst and pollutant during the optimization procedure. We assume that it can be found catalyst having efficient use in every situation but it is better to focus our attention to develop performent catalyst for certain type of pollutant such as dyes and phenols. Particularly, when the treatment of this pollutant is expensive by classical methods or the pollutant is persistent. The pollutant must be treated upstream before to be a mixture of pollutant.

References

[1] M. Schiavello (Ed.), Heterogeneous Photocatalysis, Wiley, New York, 1997.
[2] D. Bahnemann, in: P. Boule (Ed.), Handbook of Environmental Photochemistry, Springer, Berlin, 1999, p. 285.
[3] D. Bahnemann, J. Cunningham, M.A. Fox, E. Pelizzetti, P. Pichat, N. Serpone, in: G.R. Helz, R.G. Zepp, D.G. Crosby (Eds.), Aquatic and Surface Photochemistry, Lewis, Boca Raton, FL, 1994, p. 261.
[4] P. Pichat, in: G. Ert, H. Knözinger, J. Weitkamp (Eds.), Handbook of Heterogeneous Photocatalysis, Wiley, Weiheim, 1997, p. 2111.
[5] D.F. Ollis, H. Al-Ekabi (Eds.), Photocatalytic Purification and Treatment of Water and Air, Elsevier, Amsterdam, 1993.
[6] S. Malato, J. Blanco, A. Vidal, C. Richter, Appl. Catal. B: Environ. 37 (2002) 1–15.
[7] A. Fujishima, T.N. Rao, D.A. Tryk, J. Photochem. Photobio. C: Photochem. Rev. 1 (2000) 1–21.
[8] A. Mills, P. Robertson (Eds.), J. Photochem. Photobiol. A: Chem. (special issue).
[9] S. Goeringer, C.R. Chenthamarakshan, K. Rajeshwar, Electrochem. Commun. 3 (2001) 290–292.
[10] C.T.K. Thaminimulla, T. Takata, M. Hara, J.N. Kondo, K. Domen, J. Catal. 196 (2000) 362–365.
[11] Y. Bessekhouad, M. Mohammedil, M. Trari, Solar Energy Mater. Solar Cells 73 (2002) 339–350.
[12] M. Tomkiewicz, Catal. Today 58 (2000) 115–123.
[13] G. Colón, M.C. Hidalgo, J.A. Navío, Catal. Today 76 (2002) 91–101.
[14] M. Inagaki, Y. Nakazawa, M. Hirano, Y.M. Toyoda, Int. J. Inorg. Mater. 3 (2001) 809–811.
[15] Y. Zhang, G. Xiong, N. Yao, W. Yang, X. Fu, Catal. Today 68 (2001) 89–95.
[16] K.D. Kim, H.T. Kim, Powder Technol. 119 (2001) 164.
[17] Y. Bessekhouad, D. Robert, J.V. Weber, Int. J. Photoenergy, 2003, in press.
[18] K.S. Mazdiyasni, Ceram. Int. 8 (1982) 42.
[19] C. Kittel, Physique de l'état Solide, Dunod Université, 1988.
[20] J. Livage, M. Henry, C. Sanchez, Prog. Solid State Chem. 18 (1988) 259.